

# Possible therapeutic effect of combined platelet-rich plasma and stem cells on induced knee osteoarthritis in adult male albino rat: histological and immunohistochemical study

Nabila Y.A. Haleem, Mogeda M. Nasralla, Mohammed M. Abd El-Moaty, Eman F. Farid, Doaa M. Shuaib

*Department of Anatomy and Embryology, Faculty of Medicine, Cairo University, Egypt*

## SUMMARY

Osteoarthritis (OA) is a degenerative joint disease that results from breakdown of joint cartilage and underlying bone. It is the most common form of arthritis among elderly individuals. The present study aimed to investigate the effect of intra-articular injection of platelet-rich plasma (PRP) and bone marrow mesenchymal stem cells (BMSCs), both in combination and separately in the treatment of monoiodoacetate (MIA) induced OA in rats. Seventy adult male albino rats were randomly divided into seven groups, 10 rats in each (control, sham control, OA-induced, PRP, BMSCs, PRP+BMSCs and recovery). Histological examination was done using haematoxylin and eosin, alcian blue and Masson's trichrome stains. Immunohistochemical staining for collagen type II antigen and proliferating cell nuclear antigen (PCNA) was carried out. Measurements of serum interleukin 6 (IL-6) was performed using ELISA. Expression of ACAN gene was done using real-time polymerase chain reaction (PCR)

and histomorphometric measurements were analyzed. Radiographs were acquired from the knee joint. Light microscopic examination of articular cartilage (AC) from OA-induced group showed disorganization of chondrocytes, loss of zonation, pyknotic nuclei, empty lacunae and absent tidemark. There was a significant decrease in AC thickness, chondrocytes count, optical density of collagen and proteoglycan content, area percent of collagen II in the matrix in OA group compared to control and sham groups. These degenerative histomorphological alterations were associated with significant increase in serum IL-6 and decrease in ACAN gene expression. Radiographs showed narrowing of joint space and subchondral sclerosis. Intraarticular injection of PRP, BMSCs and PRP+BMSCs improved the previously mentioned alterations. Concomitant administration of PRP+BMSCs showed better effect than using PRP and BMSCs alone. In conclusion, PRP potentiated the effects of BMSCs on the repair of MIA-induced AC damage in rats. Injection of combination of

## Corresponding author:

Doaa Mahmoud Shuaib. Faculty of Medicine, Cairo University, Department of Anatomy and Embryology, Kasr Al-Ainy Street, Faculty of Medicine, 11562 Cairo, Egypt. Phone: 00201005859263. E-mail: doaa.shuaib@kasralainy.edu.eg

Submitted: July 31, 2023. Accepted: September 25, 2023

<https://doi.org/10.52083/LOAY6925>

PRP with BMSCs could be considered as a promising therapy for OA in patients.

**Key words:** Osteoarthritis – Chondrocytes – Monoiodoacetate – Platelet rich plasma – Bone marrow mesenchymal stem cells

## INTRODUCTION

Osteoarthritis (OA) is the most prevalent degenerative joint disease, which mostly impairs mobility and subsequent quality of life in elder individuals (Mehranfar et al., 2019). It affects both large and small joints of the body including the hand, feet, back, but the most commonly affected joints are hip and knee joints leading to disability (Samsonraj et al., 2017). Monoiodoacetate (MIA) is an inhibitor of glyceraldehyde-3-phosphate dehydrogenase activity and an inhibitor of glycolysis shown to induce chondrocyte death in vitro. Intra-articular injection of MIA induces chondrocyte death in the articular cartilage (AC) of rodent and non-rodent species (Pei et al., 2019).

Intra-articular injection of platelet rich plasma (PRP) is one of the current options for treatment of OA. The regenerative capacity of PRP is attributed to its high content of growth factors, which influence cartilage healing and regeneration. They include platelet-derived growth factor, transforming growth factor- $\beta$ , vascular endothelial growth factor, epidermal growth factor and insulin growth factor (Nabavizadeh et al., 2022). The use of mesenchymal stem cells is another propitious therapy of OA. The therapeutic use of MSCs is related to their anti-inflammatory activity and their capacity to differentiate into mesodermal lineages like fat, bone and cartilage (Bastos et al., 2020). Bone marrow mesenchymal stem cells (BMSCs) are the most studied and used cells in regenerative medicine (Samsonraj et al., 2017). While cell-based therapy has been shown to be hopeful for regeneration, there is a consideration that BMSCs perform better in the presence of PRP (Ahmad et al., 2020).

Although the effect of PRP and BMSCs on damaged cartilage separately is well known in the reviewed literature, studies considering the effect of their combined treatment were limited. There-

fore, the aim of the current study was to assess the histological, histomorphometric and biochemical changes in osteoarthritic cartilage of knee joint and the possible ameliorative role of PRP, BMSCs and combined PRP and BMSCs.

## MATERIAL AND METHODS

### Animals

Seventy adult male albino rats of 170-200gram body weight with apparently healthy knee joints (no swelling or limitation of movement) were obtained from the Animal and Experimental House, Faculty of Medicine, Cairo University following the guidelines for the care and use of laboratory animals (approval NO. CU-III-F-74-19). The animals were housed in groups five per cage measuring 41×28×19 cm and allowed to standardized laboratory diet and water ad libitum throughout the experiment.

### Chemicals

*Mono-iodoacetate:* It was purchased from Sigma-Aldrich Chemie GmbH (Sigma, St. Louis, MO, USA; cat #12512) in the form of powder. A total amount of 30 mg of MIA powder was dissolved in 15 ml phosphate buffered saline solution (Guzman et al., 2003).

*Phosphate buffered saline (PBS):* It is a water-based salt solution containing disodium hydrogen phosphate, sodium chloride, potassium chloride and potassium dihydrogen phosphate. It helps to maintain a constant PH.

*Platelet rich plasma:* An autologous PRP was freshly prepared and was injected within one hour after preparation in the form of 30 $\mu$ l of PRP dissolved in 20 $\mu$ l PBS intra-articular in the right knee joints of rats (Mifune et al., 2013). They were obtained from the Biochemistry Department, Faculty of Medicine, Cairo University.

*Bone-marrow derived Mesenchymal stem cells:* Isolation, culture and labeling of BMSCs were performed in Molecular Biology Unit, Biochemistry Department, Faculty of Medicine, Cairo University. According to Institutional Animal Care and Use Committee guidelines, 12 weeks old rats were sacrificed under chloroform anesthesia. The fe-

mur and tibia were removed under aseptic conditions and cancellous bone was removed and washed with PBS 4 or 5 times. Bone marrows were cleaned out using Dulbecco's Modified Eagle's media (DMEM) and media were changed every 3 to 4 days (Smajilagić et al., 2013). When huge colonies formed, cultures were rinsed twice with PBS and trypsin was added to cells (0.25% trypsin in 1ml Ethylene Diamine Tetra Acetate (EDTA)) for 5 minutes at 37°C. After centrifugation, cell pellets were resuspended with serum-supplemented medium and incubated in 25 cm<sup>3</sup> culture flasks (Alhadlaq and Mao, 2004). The BMSCs in the culture were identified by their plastic adhesiveness and fusiform shape (Aziz et al., 2007). To track the migration and homing of BMSCs at the site of intra-articular injection, cultured cells were labeled with fluorescent cell tracker PKH26 (Sigma, USA, MINI26) according to manufacturer's instructions (Kyriakou et al., 2008).

### Experimental design

The animals were randomly divided into seven groups (ten rats in each) according to lottery randomization method (Singh and Masuku, 2014). Seven cards were prepared with labels representing the different groups. The cards were placed in a container and shuffled thoroughly. Each card was drawn one by one blindly from the container and each rat was assigned to the corresponding group based on the label on the card. This process was repeated until all rats had been assigned to the groups.

Group I (Control group): The rats were housed without any manipulation or medications. They were then subdivided into two subgroups:

Subgroup Ia: Consisted of five rats. They were sacrificed after two weeks from the onset of the experiment.

Subgroup Ib: Consisted of five rats. They were sacrificed after six weeks from the onset of the experiment.

Group II (Sham control group): The animals were injected intra-articular with a single dose of 0.5 ml of PBS through infrapatellar ligament of the right knee joint. They were then subdivided into two subgroups:

Subgroup IIa: Five rats were sacrificed after two weeks from the onset of the experiment.

Subgroup IIb: Five rats were sacrificed after six weeks from the onset of the experiment.

Group III (OA-induced group): The rats received a single intra-articular injection of 1 mg of MIA dissolved in 0.5 ml of PBS through infrapatellar ligament of the right knee joint and sacrificed two weeks after the injection (Guzman et al., 2003).

Group IV (PRP- treated group): They received single intra-articular injection of 30µl of PRP dissolved in 20µl PBS through infrapatellar ligament of the right knee joint two weeks after injection of MIA. The animals were sacrificed four weeks later (Mifune et al., 2013).

Group V (BMSCs- treated group): They received single intra-articular injection of 5.0X10<sup>5</sup> BMSCs resuspended in 50µl PBS through infrapatellar ligament of the right knee joint two weeks after injection of MIA, then were sacrificed four weeks later (Mifune et al., 2013).

Group VI (PRP+BMSCs-treated group): The rats received a single intra-articular injection of a combination of 30µl PRP dissolved in 20µl PBS and 5.0 X10<sup>5</sup> BMSCs through infrapatellar ligament of the right knee joint two weeks after injection of MIA. They were sacrificed after four weeks (Mifune et al., 2013).

Group VII (Recovery group): The rats received a single intra-articular of 1 mg of MIA dissolved in 0.5 ml of PBS through infrapatellar ligament of the right knee joint and were sacrificed six weeks after the injection (Matsumoto et al., 2009).

The animals subjected for intra-articular injection underwent general anesthesia by ether inhalation. The area surrounding the knee joint was trimmed and wiped with alcohol. The patellar ligament was seen as white line below patella. The knee joint was kept in a bent position and the drug was injected in the gap below the patella at a 90° angle using insulin syringe (Pitcher et al., 2016).

All animals were anesthetized by mild ether inhalation at the allocated time of each group, then sacrificed by intraperitoneal injection of phenobarbitone sodium (80µg/g). The femoral condyles of the right knee joint were dissected and fixed in

10% buffered formalin solution. The specimens were decalcified using EDTA. After changing the solution daily for six weeks, the specimens were subjected to the following:

### Histological study

The specimens were dehydrated in ascending grades of alcohol, cleared in xylene, embedded in paraffin and sagittal sections of 5  $\mu\text{m}$  thickness were cut and stained by:

- *Haematoxylin and eosin (H&E)*: For routine histological examination (Kiernan, 2001).
- *Alcian blue*: For detection of proteoglycan in chondrocytes (Bancroft and Gamble, 2008).
- *Masson's trichrome*: For detection of collagen content in the matrix (Bancroft & Gamble, 2008).
- *Immunohistochemical staining for collagen type II antigen* (Bancroft & Gamble, 2008): Primary antibody: Collagen II Ab-3 (Clone 6B3): It is a mouse monoclonal antibody (thermo-scientific, CA 94538, USA, catalogue number MS-306-R7) at dilution 1:200 for detection of type II collagen.
- *Immunohistochemical staining for Proliferating Cell Nuclear antigen (PCNA)*: Primary antibody: The PC10 monoclonal antibody (clone PC10, M0879): It is a mouse monoclonal antibody (Dako company, Cairo, Egypt, Catalog No.IMG.144A) at a dilution 1:100 was used for detection of cell proliferation.

### Histomorphometric study

Five non-overlapping high power fields (x400) from five sections (from each rat) of 10 rats per group were randomly chosen. The measurements were obtained using "Leica Qwin 500 C" image analyzer computer system Ltd. (Cambridge, England).

The following parameters were measured:

- Articular cartilage thickness in H&E-stained sections ( $\mu\text{m}$ ). Four measures were taken and the average was calculated for each slide.
- Optical density of proteoglycan content of chondrocytes in alcian blue stained sections.
- Optical density of collagen content of cartilage matrix in Masson's trichrome stained sections.

- Area percent of collagen II immunopositive matrix in collagen II-stained sections. Optical density of proteoglycan content of chondrocytes, collagen content of the matrix and area percent of collagen II immunopositive matrix were done by transforming the colored images into grey images then masking the positive areas by a red binary color using image analyzer software.
- Chondrocytes count in PCNA stained-sections. It was done by using counting cells tool in image analysis software.

### Biochemical study

*ELISA*: Three ml blood was obtained from the rat's tail and collected in heparinized tubes for biochemical determination of serum level of IL-6 by an ELISA kit as described in manufacturer's instructions (R&D Systems, Inc., Minneapolis, MN).

### Quantitative analysis of ACAN gene by real time polymerase chain reaction (RT-PCR):

**Total RNA extraction:** Articular cartilage was harvested and grounded by a mortar and pestle in liquid nitrogen. Extraction of RNA was done by homogenization in TRIzol reagent (Invitrogen, Life Technologies, USA) according to the instructions of the manufacturer. The RNA concentrations and purity were measured with an ultraviolet spectrophotometer.

**Complementary DNA (cDNA) synthesis:** The cDNA was synthesized from 1  $\mu\text{g}$  RNA using Superscript III First-Strand Synthesis; a system described in the manufacturer's protocol (Invitrogen, Life Technologies). One  $\mu\text{g}$  of total RNA was mixed with 50  $\mu\text{M}$  oligo (DT) 20, 50 ng/ $\mu\text{L}$  random primers, and 10 mM dNTP mix in a total volume of 10  $\mu\text{L}$ . The mixture was incubated at 56  $^{\circ}\text{C}$  for five minutes, and then placed on ice for three minutes. The reverse transcriptase master mix containing 2  $\mu\text{L}$  of 10 $\times$  RT buffer, 4  $\mu\text{L}$  of 25 mM  $\text{MgCl}_2$ , 2  $\mu\text{L}$  of 0.1 M DTT, and 1  $\mu\text{L}$  of SuperScript III RT (200 U/ $\mu\text{L}$ ) was added to the mixture and was incubated at 25  $^{\circ}\text{C}$  for ten minutes followed by 50 minutes at 50  $^{\circ}\text{C}$ .

**Real time quantitative PCR:** The relative abundance of mRNA species was assessed using the SYBR Green method on an ABI prism 7500 se-

quence detector system (Applied Biosystems, Foster City, CA). Primers were designed with Gene Runner Software (Hasting Software, Inc., Hasting, NY) from RNA sequences from Gene Bank. Quantitative RT-PCR was performed in a 25- $\mu$ l reaction volume consisting of 2X SYBR Green PCR. Master Mix (Applied Biosystems), 900 nM of each primer and 2-3  $\mu$ l of cDNA. Amplification conditions were 2 min. at 50°, 10 min. at 95° and 40 cycles of denaturation for 15 seconds and annealing/extension at 60° for 10 min. Data from real-time assays were calculated using the v1.7 Sequence Detection Software from PE Biosystems (Foster City, CA). Relative expression of studied gene mRNA was calculated using the comparative Ct method. All values were normalized to the beta actin gene and reported as fold change.

The primer sequence of the ACAN was:

F: 5'- AGATGGCACCTCCGATACC -3' R: 3'- GACACCTCGGAAGCAGAA -5'

### Radiographic evaluation

The procedure was performed at Faculty of Veterinary Medicine, Cairo University. It was carried out immediately after euthanasia before rigor mortis. A dental radiography periapical film unit was used. Radiographs were made in dorsoplantar position at full extension. The images were analyzed by a radiologist without knowledge of groups of animals evaluated (Morais et al., 2016).

### Statistical analysis

The quantitative data were tabulated and subjected to statistical analysis using SPSS (statistical package for social science) version 21. The numerical data was described as mean  $\pm$  standard deviation (SD). The statistical significance of the difference between all the obtained mean values will be assessed using one way ANOVA test. The Bonferroni post hoc test was applied to compare different groups. The probability level (p-value)  $\geq$  0.05 was considered significant.

## RESULTS

### Histological and histomorphometric results

Histological examination of AC sections from control group (subgroup Ia and Ib) and sham

group (subgroup IIa and IIb) showed similar findings, therefore, they were discussed together.

**Haematoxylin and eosin-stained sections:** Examination of H&E-stained sections from control group (subgroup Ia and Ib) and sham group (subgroup IIa and IIb) showed normal morphological architecture with regular histological zones of AC. The superficial zone exhibited flat chondrocytes and the transitional zone was formed of rounded chondrocytes with rounded nuclei inside lacuna arranged in cell nests (composed of 2-4 chondrocytes). In the deep zone, chondrocytes were arranged in columns perpendicular to the surface of the cartilage. The tidemark appeared as a basophilic line separating the deep zone from underlying calcified zone (Fig. 1a). On the other hand, degenerative histomorphological alterations were observed in OA-induced group in the form of loss of zonation, faint or absent tidemark, disorientation of chondrocytes and presence of ghost cells. Empty lacune with pyknotic nuclei were observed. The articular surface showed exfoliation of superficial zone (Fig. 1b).

Histomorphological improvement was observed in PRP-treated group. Regular articular surface, flat chondrocytes and cell nests were seen in the superficial zone and transitional zones respectively. However, cell columns could not be detected in the deep zone and tidemark was absent (Fig.1c). In BMSCs-treated group, zonal organization was detected apart from absent columns in the deep zone. In addition to obvious tidemark (Fig. 1d). In group VI, concomitant administration of PRP+BMSCs significantly alleviated MIA-induced AC alterations as evidenced by better zonal organization with reappearance of columns in the deep zone. However, the tidemark was faint (Fig. 1e). Moreover, there was no further improvement in recovery group, which showed loss of zonation, disorientation of chondrocytes, absent tidemark. In addition to the presence of clefts and pyknotic nuclei (Fig. 1f).

Statistically significant decrease in the mean AC thickness was observed in OA- induced group compared to control (p<.001\*) and sham groups (p<.001\*). Meanwhile, PRP, MSCs and concomitant PRP+MSCs groups showed a significant increase in the mean AC thickness compared to

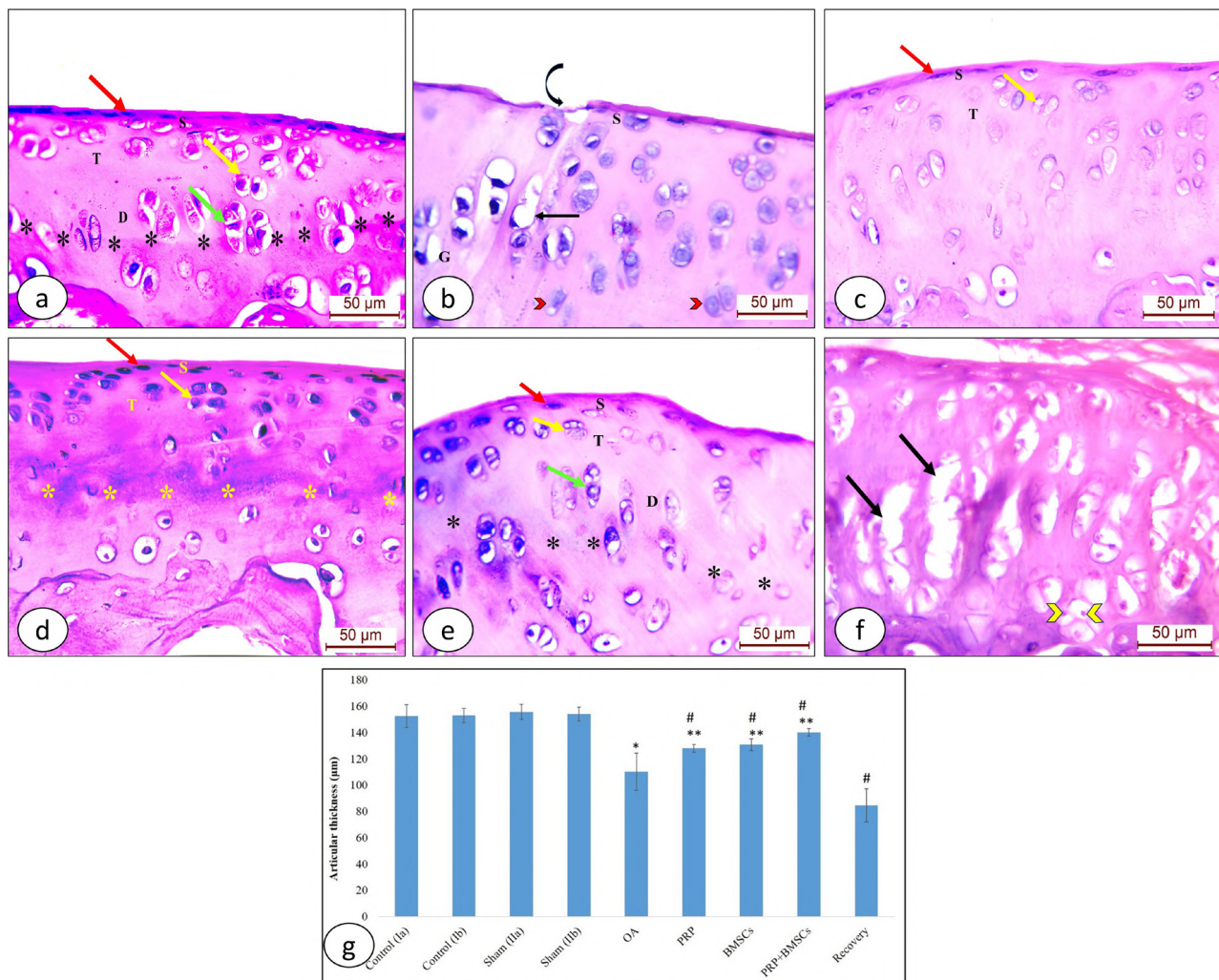


**Fig. 1.-** H&E-stained sections from rat AC of different groups (x400): **(a)** Sham control group shows normal architecture; elongated flat chondrocytes (red arrow) are shown in the superficial zone (S). The transitional zone (T) reveals rounded chondrocytes in cell nests (yellow arrow). The deep zone (D) displays chondrocytes arranged in columns (green arrow). The tidemark (\*) is illustrated. **(b)** Section from OA-induced group demonstrates degenerative histomorphological alterations with loss of zonation, abnormal distribution of cells (arrowheads), exfoliation (curved arrow) in the superficial zone (S) and absent tidemark. Note presence of ghost cell (G). Empty lacuna with pyknotic eccentric nucleus is illustrated (arrow). **(c)** In PRP-treated group, flat chondrocytes (red arrow) and cell nests (yellow arrow) are shown in the superficial (S) and transitional (T) zones respectively. Cell columns and tidemark are absent. **(d)** BMSCs-treated group displays flat chondrocytes (red arrow) in the superficial zone (S) and cell nests (yellow arrow) in the transitional zone (T). Cell columns are absent. The tidemark (\*) is shown. **(e)** In group VI, concomitant administration of PRP+BMSCs demonstrates regular articular surface. Flat chondrocytes (red arrow), cell nests (yellow arrow) and cell columns (green arrow) are illustrated in the superficial (S), transitional (T) and deep (D) zones respectively. Faint tidemark (\*) is shown. **(f)** Loss of zonation, disorientation of chondrocytes, clefts (arrows) and pyknotic nuclei (arrowheads) are illustrated in recovery group. The tidemark is absent. **(g)** Mean AC thickness in different groups: \* ( $p < .05$ ) vs control group, # ( $p < .05$ ) vs OA, \*\* ( $p < .05$ ) vs recovery. Scale bars: 50  $\mu\text{m}$ .

OA-induced group ( $p = .041^*$ ,  $.008^*$  and  $< .001^*$  respectively). However, the difference in the mean AC thickness between PRP, MSCs and concomitant PRP+MSCs groups was statistically non-significant. Regarding recovery group, a statistically significant decrease in AC thickness was found compared to OA ( $p < .001^*$ ), PRP ( $p = .041^*$ ), MSCs ( $p < .001^*$ ) and concomitant PRP+MSCs ( $p < .001^*$ ) treated groups (Fig. 1g) (Table 1).

**Alcian blue-stained sections:** In alcian blue-stained sections, chondrocytes were deeply

stained in control group (subgroup Ia and Ib) and sham group (subgroup IIa and IIb) (Fig. 2a). However, most of chondrocytes exhibited faint alcian blue staining in OA-induced group (Fig. 2b). Improvement was detected in PRP, BMSCs, as well as PRP+BMSCs-treated groups as most of chondrocytes were moderately stained by alcian blue (Figs. 2c, d, E). Faint alcian blue staining was observed in AC sections from recovery group (Fig. 2f).

Regarding the mean optical density of proteoglycan content in alcian blue-stained sections, there

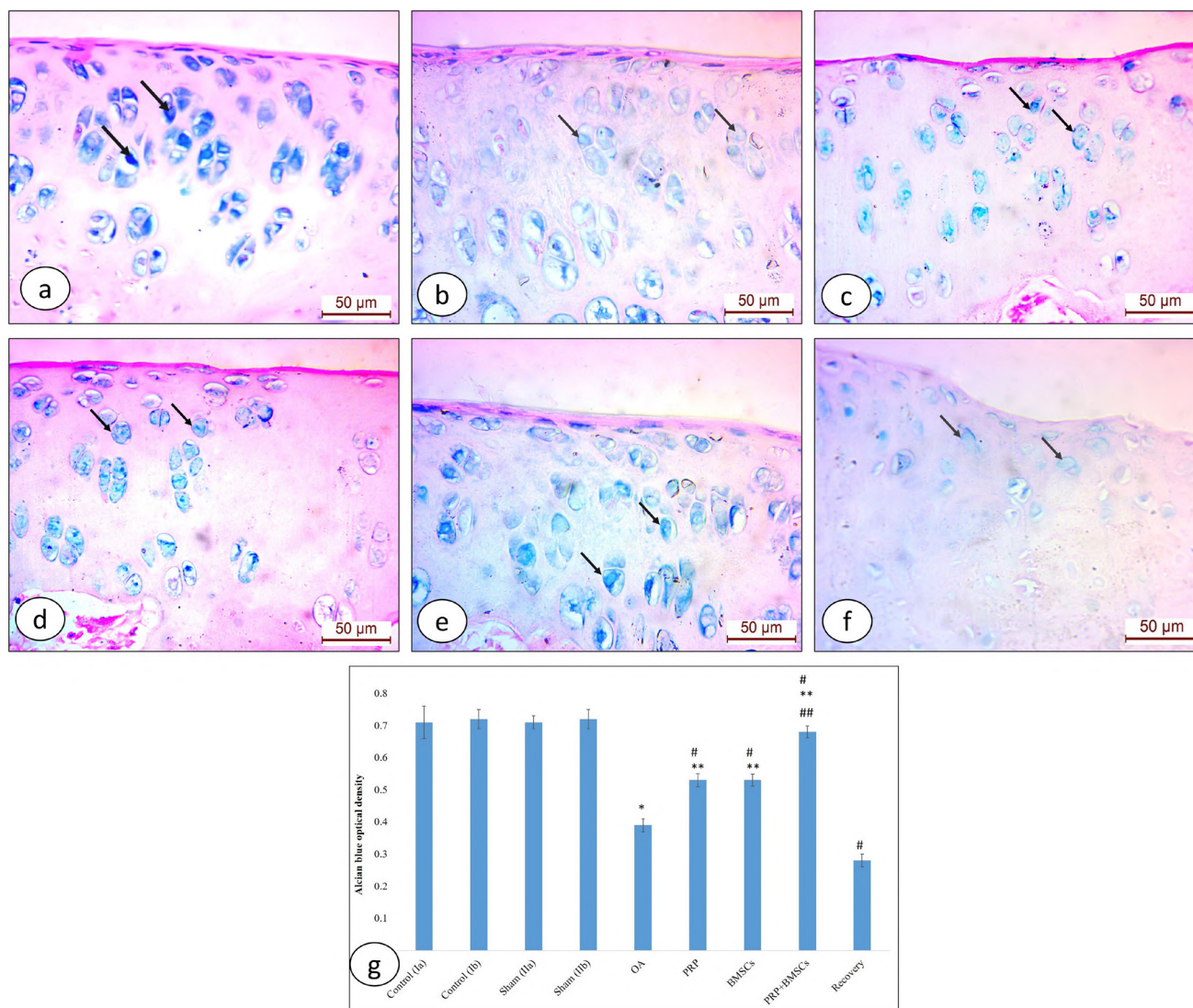


**Fig. 2.-** Alcian blue-stained sections from rat AC of different groups (x400): **(a)** Deep blue stained chondrocytes are shown in sham group (arrows). **(b)** OA-induced group reveals light blue stained chondrocytes (arrows). **(c, d, e)** Moderately stained chondrocytes are illustrated in PRP, BMSCs and concomitant PRP+BMSCs treated groups (arrows). **(f)** In recovery group, light blue stained chondrocytes are demonstrated (arrows). **(g)** Mean optical density of proteoglycan content of chondrocytes in AC in different groups: \* ( $p < .05$ ) vs control group, # ( $p < .05$ ) vs OA, \*\* ( $p < .05$ ) vs recovery, ## ( $p < .05$ ) vs PRP group and BMSCs group. Scale bars: 50  $\mu$ m.

was significant decrease in OA-induced group compared to control ( $p < .001^*$ ) and sham groups ( $p < .001^*$ ). A statistically significant increase in the mean optical density in PRP ( $p < .001^*$ ), MSCs ( $p < .001^*$ ) and concomitant PRP+MSCs ( $p < .001^*$ ) groups was found compared to OA-induced group. Moreover, there was significant increase in the optical density in concomitant PRP+MSCs group compared to PRP ( $p < .001^*$ ) and MSCs ( $p < .001^*$ ) groups indicating better response. Regarding recovery group, the mean optical density showed a significant decrease compared to OA ( $p < .001^*$ ), PRP ( $p < .001^*$ ), MSCs ( $p < .001^*$ ) and concomitant PRP+MSCs ( $p < .001^*$ ) groups (Fig. 2g) (Table 1).

**Masson's trichrome-stained sections:** Regarding control group (subgroup Ia and Ib) and sham group (subgroup IIa and IIb), examination of Masson's trichrome-stained sections exhibited deeply stained basophilic matrix by large amount of collagen (Fig. 3a). Decreased collagen was observed in OA-induced group in the form of areas of mild to moderate basophilic staining (Fig. 3b). In PRP-treated group, the matrix showed moderate basophilic staining (Fig. 3c), while in BMSCs-treated group, moderate to deep basophilic staining of matrix was detected (Fig. d). Combined PRP+BMSCs treated group exhibited deeply stained basophilic matrix indicating increased collagen (Fig. e). Examination of sections

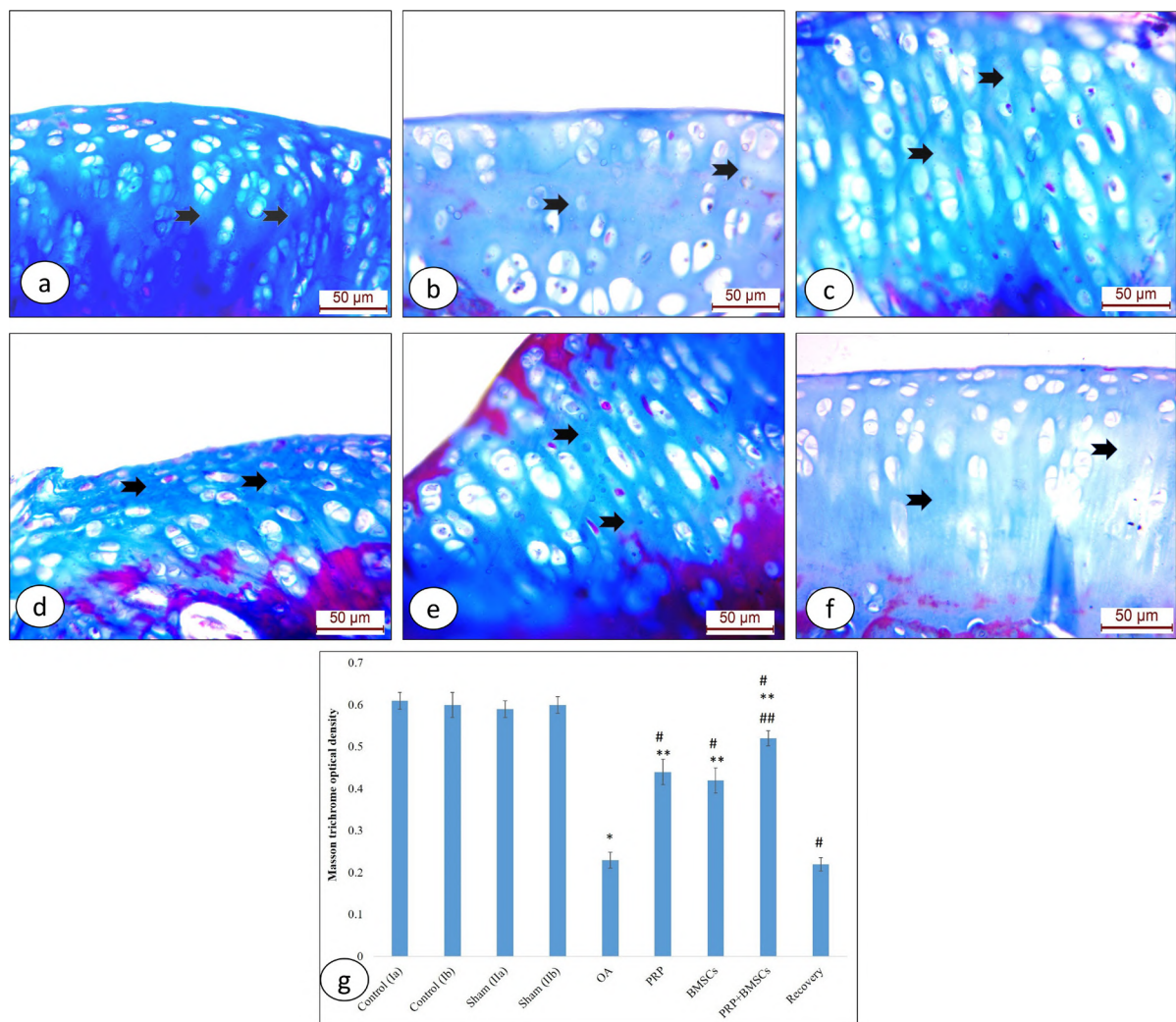


**Fig. 3.-** Masson's trichrome-stained sections from rat AC of different groups (x400): **(a)** Sham control group shows deeply stained basophilic matrix between chondrocytes. (arrows). **(b)** Mild to moderate basophilic staining of matrix is demonstrated in OA-induced group (arrows). **(c)** Matrix shows moderate basophilic staining in PRP-treated group (arrows). **(d)** In BMSCs-treated group, moderate to deep basophilic staining of matrix is illustrated (arrows). **(e)** PRP+BMSCs cotreatment group displays deeply stained basophilic matrix (arrows). **(f)** Mildly stained basophilic matrix is shown in recovery group (arrows). **(g)** Mean optical density of collagen content in the matrix of AC in different groups: \* ( $p < .05$ ) vs control group, # ( $p < .05$ ) vs OA, \*\* ( $p < .05$ ) vs recovery, ## ( $p < .05$ ) vs PRP group and BMSCs group. Scale bars: 50 µm.

**Table 1.** Mean values of AC thickness, optical density of proteoglycan content, optical density of collagen content, area percent of collagen II and chondrocytes count in all rat groups.

Groups	Articular cartilage thickness (µm) (Mean± SD)	Optical density of proteoglycan content (Mean± SD)	Optical density of collagen content (Mean± SD)	Area percent of collagen II (Mean± SD)	Chondrocytes count (Mean± SD)
Ia (Control group)	152.7 ± 8.6	0.71 ± .05	0.61 ± .02	58.6 ± 2.3	50.2 ± 1.9
Ib (Control group)	153.1 ± 5.4	0.72 ± .03	0.60 ± .03	57.5 ± 1.9	50.6 ± 3
IIa (Sham control group)	155.7 ± 5.7	0.71 ± .02	0.59 ± .02	56.4 ± 1.2	47.8 ± 1.4
IIb (Sham control group)	154.2 ± 5.2	0.72 ± .03	0.60 ± .02	56.9 ± 1.4	49.6 ± 2.7
III (OA-induced group)	110.2 ± 14.2	0.39 ± .02	0.23 ± .019	28.1 ± 1.8	23 ± 2.7
IV (PRP-treated group)	128.1 ± 2.9	0.53 ± .02	0.44 ± .03	34.8 ± 1.0	36.2 ± 3.3
V (MSCs-Treated group)	130.9 ± 4.5	0.53 ± .019	0.42 ± .03	41.02 ± 0.9	38 ± 1.8
VI (PRP+BMSCs-treated group)	140.2 ± 2.7	0.68 ± .018	0.52 ± .018	48.6 ± 2.6	44.2 ± 1.9
VII (Recovery group)	84.6 ± 12.6	0.28 ± .02	0.22 ± .016	18 ± 0.8	13.2 ± 1.6

SD: Standard deviation, OA: Osteoarthritis, PRP: Platelet rich plasma, BMSCs: Bone marrow mesenchymal stem cells

from recovery group revealed mild staining of matrix reflecting decreased collagen (Fig. 3f).

The mean optical density of collagen content in the matrix of AC in OA-induced group showed significant decrease compared to control ( $p < .001^*$ ) and sham groups ( $p < .001^*$ ). Regarding PRP, MSCs and PRP+BMSCs treated groups, a statistically significant increase of the optical density was recognized compared to OA-induced group ( $p < .001^*$  in the three groups). Further improvement was found in PRP+BMSCs treated group as evident by the significant increase in the optical density compared to PRP ( $p < .001^*$ ) and MSCs ( $p < .001^*$ ) treated groups (Fig. 3g). Furthermore, a statistically significant decrease in the optical density was detected in recovery group compared to OA ( $p < .001^*$ ), PRP ( $p < .001^*$ ), MSCs ( $p < .001^*$ ) and PRP+BMSCs ( $p < .001^*$ ) treated groups (Fig. 3g) (Table 1).

**Collagen II immune-stained sections:** Examination of collagen II-stained sections of control group (subgroup Ia and Ib) and sham group (subgroup IIa and IIb) showed strong extracellular immunoreactivity in the superficial zone, moderate immunoreactivity in the transitional zone and mild to moderate immunoreactivity of the deep zone. Collagen bundles were seen (Fig. 4a). In OA-induced group, weak extracellular immunoreactivity with patchy appearance was observed (Fig. 4b). Examination of sections from PRP and BMSCs treated groups exhibited strong immunostaining in the superficial zone and moderate staining in the transitional zone. Patches of collagen fibers were detected in the deep zone (Figs. 4c, d). In group VI (PRP+BMSCs concomitant administration), there was an increase in collagen II immunoreactivity with strong immunostaining in the superficial zone, moderate staining in the transitional zone and mild staining of deep zone. Moreover, collagen bundles were observed in this group (Fig. 4e). Sections of group VII (recovery group) revealed weak extracellular immunoreactivity of collagen II (Fig. 4f).

The mean area percent of collagen II revealed a significant decrease in OA-induced group in comparison to control ( $p < .001^*$ ) and sham groups ( $p < .001^*$ ) (Fig. 4g). In PRP, MSCs and PRP+BMSCs treated groups, a statistically significant increase

in the mean area percent was found compared to OA-induced group ( $p < .001^*$  in the three groups) (Fig. 4g). Also, concomitant PRP+BMSCs administration showed a significant increase in the mean area percent compared to PRP ( $p < .001^*$ ) and MSCs ( $p < .001^*$ ) groups (Fig. 4g). When comparing recovery group to OA, PRP, MSCs and PRP+BMSCs treated groups, a significant decrease in the mean area percent was found ( $p < .001^*$  in the four groups) (Fig. 4g) (Table 1).

**PCNA-immunostained sections:** Abundant proliferating chondrocytes were detected in PCNA-stained sections from control group (subgroup Ia and Ib) as well as sham group (subgroup IIa and IIb) (Fig. 5a). On the other hand, few chondrocytes were detected in OA-induced group (Fig. 5b). Abundant proliferating chondrocytes were detected in PRP, BMSCs and concomitant PRP+BMSCs treated groups (Figs. 5c, d, e). Sections of AC from recovery group showed few chondrocytes (Fig. 5f).

Regarding chondrocytes count, there was a significant decrease in OA-induced group compared to control ( $p < .001^*$ ) and sham ( $p < .001^*$ ) groups. While in PRP, MSCs and PRP+BMSCs treated groups, a statistically significant increase was found compared to the OA-induced group ( $p < .001^*$  in the three groups). Moreover, there was a statistically significant increase in the chondrocyte count in PRP+BMSCs treated group compared to PRP and MSCs groups ( $p < .001^*$ ,  $< .008^*$  respectively) indicating further improvement. When comparing recovery group to OA, PRP, MSCs and PRP+BMSCs treated groups, a statistically significant decrease in chondrocytes count was observed ( $p < .001^*$  in the four groups) (Fig. 5g) (Table 1).

## Biochemical results

**Determination of serum level of IL-6:** The level of the proinflammatory cytokine interleukin IL-6 was measured in the serum of rats from different groups. A significant increase in the mean serum IL6 level was found in OA-induced group in comparison to control ( $p < .001^*$ ) and sham ( $p < .001^*$ ) groups. Treatment with PRP, MSCs as well as PRP and BMSCs concomitantly resulted in a significant reduction in IL-6 levels compared to OA-induced

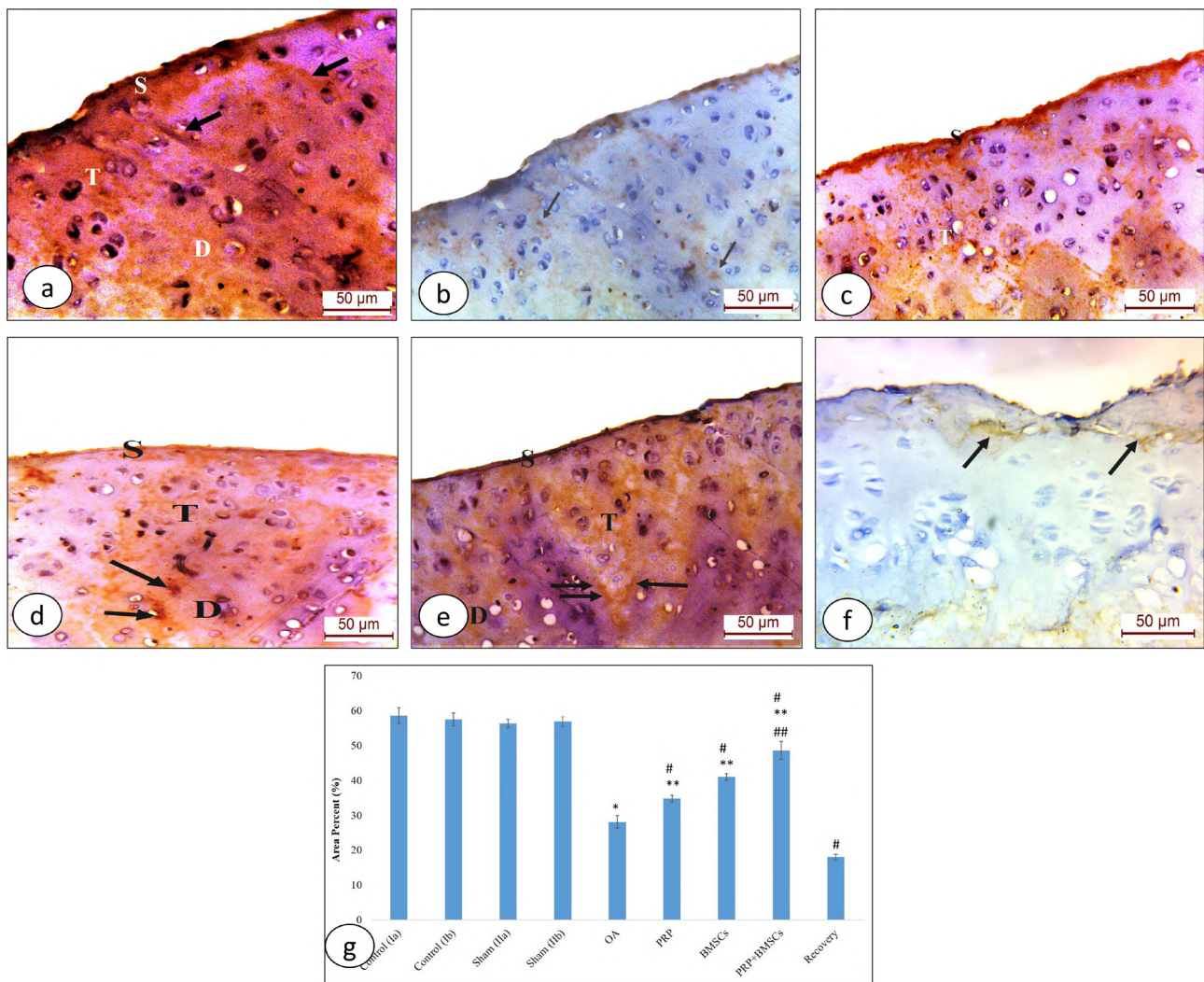


**Fig. 4.-** Anti collagen II immunostained sections from rat AC of different groups (x400): **(a)** Sham control group shows strong extracellular immunoreactivity in the superficial zone (S), moderate immunoreactivity in the transitional zone (T) and mild to moderate immunoreactivity in deep zone (D). Collagen bundles (arrows) are shown. **(b)** Weak extracellular immunoreactivity of collagen II with patchy appearance is detected in OA-induced group (arrows). **(c)** Strong immunoreactivity in the superficial zone (S) and moderate staining of the transitional zone (T) are demonstrated in PRP-treated group. **(d)** BMSCs-treated group exhibits strong immunoreactivity in the superficial zone (S) and moderate staining in the transitional zone (T). Patches of collagen fibers (arrows) are shown in the deep zone (D). **(e)** Concomitant administration of PRP+BMSCs in group VI displays strong immunoreactivity in the superficial zone (S), moderate staining in the transitional zone (T) and mild staining in the deep zone (D). Collagen bundles are shown (arrows). **(f)** In recovery group, weak extracellular immunoreactivity of collagen II is demonstrated (arrows). **(g)** Mean area percent of collagen II content of cartilage matrix in different groups: \* ( $p < .05$ ) vs control group, # ( $p < .05$ ) vs OA, \*\* ( $p < .05$ ) vs recovery, ## ( $p < .05$ ) vs PRP group and BMSCs group. Scale bars: 50  $\mu$ m.

group ( $p < .001^*$  in the three groups). Moreover, better therapeutic effect was found with PRP and BMSCs coadministration as a significant decrease in IL6 level was found in this group compared to PRP ( $p < .001^*$ ) and MSCs groups ( $p < .001^*$ ). Considering recovery group, a significant increase in the level of IL6 was observed in comparison with OA ( $p < .001^*$ ), PRP ( $p < .001^*$ ), MSCs ( $p < .001^*$ ) and PRP+BMSCs ( $p < .001^*$ ) treated groups (Fig. 6) (Table 2).

**Expression of ACAN gene in the AC:** When compared with control and sham groups, MIA administration in OA-induced group resulted in a significant de-

crease in ACAN gene expression ( $p < .001^*$ ). In PRP, MSCs and PRP+BMSCs treated groups, there was a statistically significant increase in ACAN gene expression compared to OA-induced group ( $p < .001^*$  in the three groups). Concomitant administration of PRP and BMSCs in group VI resulted in a considerable upregulation in the expression of ACAN gene when compared to PRP ( $p < .001^*$ ) and MSCs ( $p < .001^*$ ) groups. Recovery from MIA resulted in a statistical drop in the expression of ACAN gene when compared to OA ( $p < .001^*$ ), PRP ( $p < .001^*$ ), MSCs ( $p < .001^*$ ) and PRP+BMSCs ( $p < .001^*$ ) treated groups (Fig. 7) (Table 2).

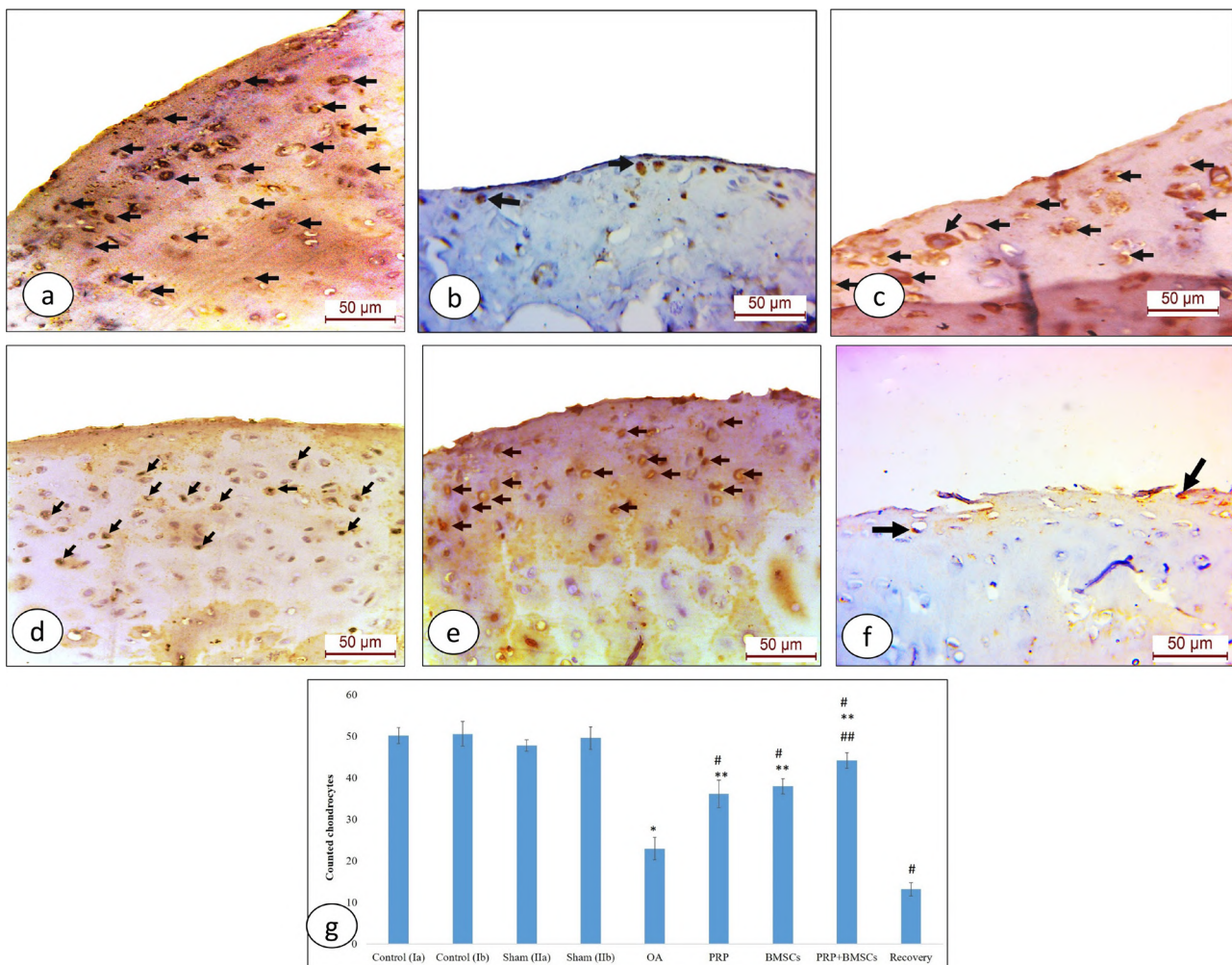


**Fig. 5.-** PCNA immunostained sections from rat AC of different groups (x400): **(a)** Abundant proliferating chondrocytes are illustrated in control group (arrows). **(b)** OA-induced group exhibits few proliferating chondrocytes (arrows). **(c, d, e)** Abundant chondrocytes are demonstrated in PRP, BMSCs and concomitant PRP+BMSCs treated groups (arrows). **(f)** Recovery group shows few chondrocytes (arrows). **(g)** Mean chondrocytes count in AC in all groups: \* ( $p < .05$ ) vs control group, # ( $p < .05$ ) vs OA, \*\* ( $p < .05$ ) vs recovery, ## ( $p < .05$ ) vs PRP group and BMSCs group. Scale bars: 50  $\mu$ m.

**Table 2.** Mean values of inflammatory marker IL-6 (pg/ml) in serum and ACAN gene expression articular cartilage tissue in all rat groups.

Groups	IL6 (pg/ml) (Mean $\pm$ SD)	ACAN gene expression (Mean $\pm$ SD)
Ia (Control group)	33.6 $\pm$ 1.3	1.05 $\pm$ .03
Ib (Control group)	33.3 $\pm$ 1.2	1.06 $\pm$ .02
IIa (Sham control group)	33.1 $\pm$ 2.2	1.08 $\pm$ .06
IIb (Sham control group)	33.5 $\pm$ 2.6	1.06 $\pm$ .08
III (OA-induced group)	96.2 $\pm$ 1.5	.3 $\pm$ .04
IV (PRP-treated group)	71.9 $\pm$ 3.5	.7 $\pm$ .03
V (MSCs-Treated group)	50.7 $\pm$ 1.6	.7 $\pm$ .03
VI (PRP+BMSCs-treated group)	41.6 $\pm$ 1.6	.9 $\pm$ .02
VII (Recovery group)	124.5 $\pm$ 4.5	.2 $\pm$ .04

SD: Standard deviation, OA: Osteoarthritis, PRP: Platelet rich plasma, BMSCs: Bone marrow mesenchymal stem cells

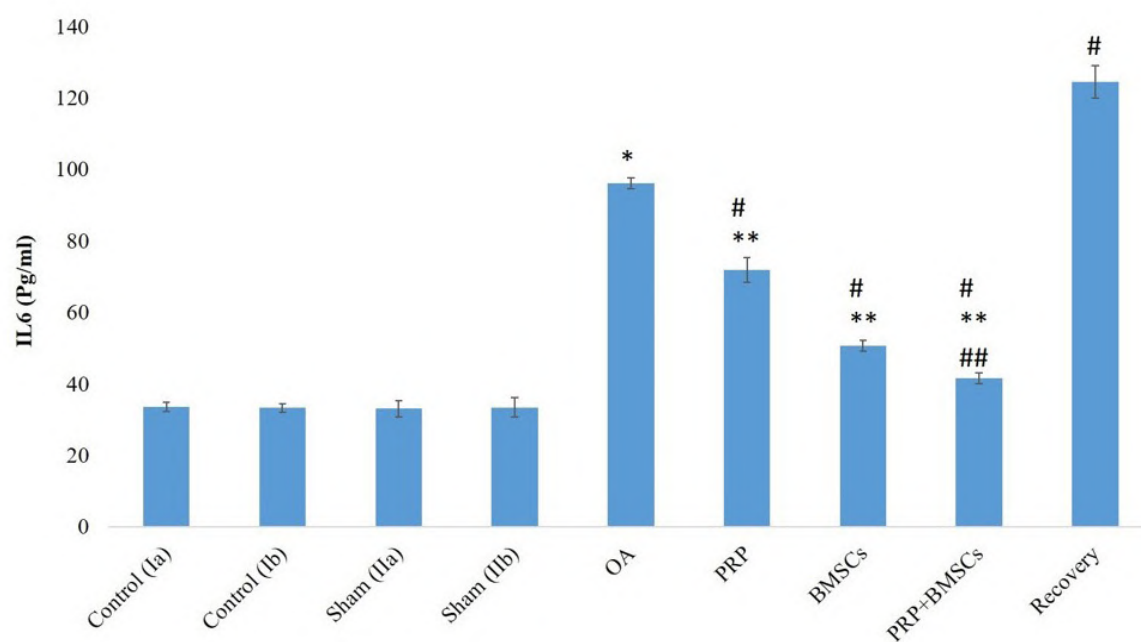


**Fig. 6.-** Mean level of serum IL-6 in different groups: \* ( $p < .05$ ) vs control group, # ( $p < .05$ ) vs OA, \*\* ( $p < .05$ ) vs recovery, ## ( $p < .05$ ) vs PRP group and BMSCs group.

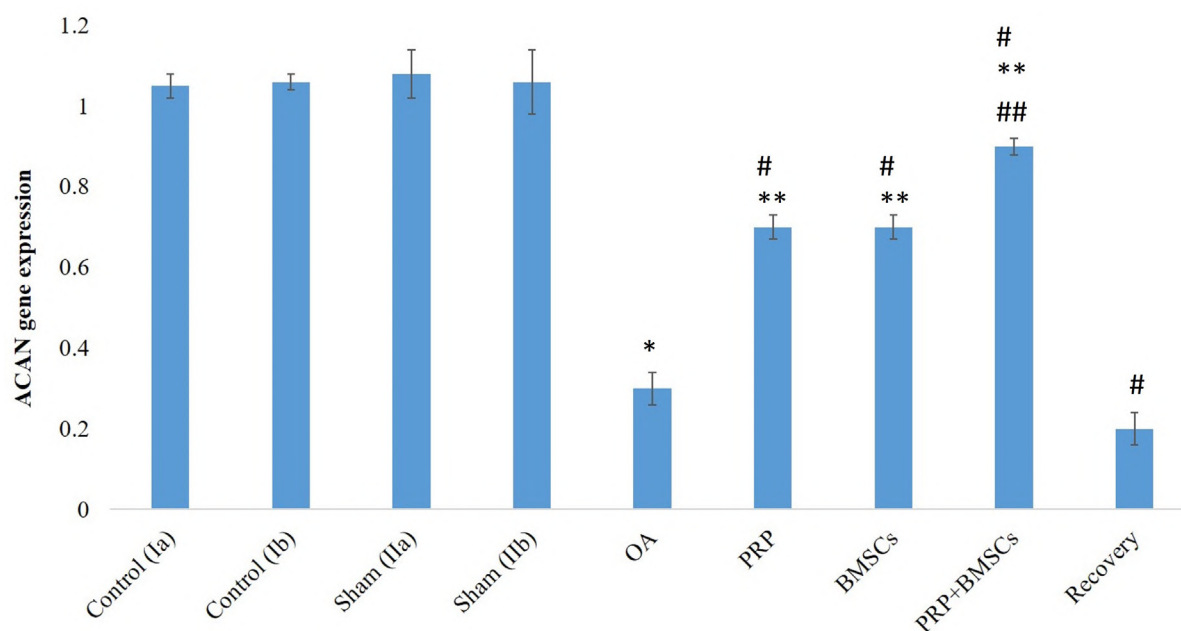


**Fig. 7.-** Mean level of ACAN gene expression in different groups: \* ( $p < .05$ ) vs control group, # ( $p < .05$ ) vs OA, \*\* ( $p < .05$ ) vs recovery, ## ( $p < .05$ ) vs PRP group and BMSCs group.

### Radiographic results

Radiographs of the knee joint from control and sham groups demonstrated a regular articular surface with normal tibiofibular joint space. No osteophytes were detected (Fig. 8a). On the other hand, X-rays of the knee joint from OA-induced

groups showed narrowed tibiofibular joint space compartment, irregular tibial articular surface, subchondral sclerosis and minute marginal osteophytes (Fig. 8b). Improvement of joint space was observed in radiographs from PRP, BMSCs and concomitant treatment groups with no mar-

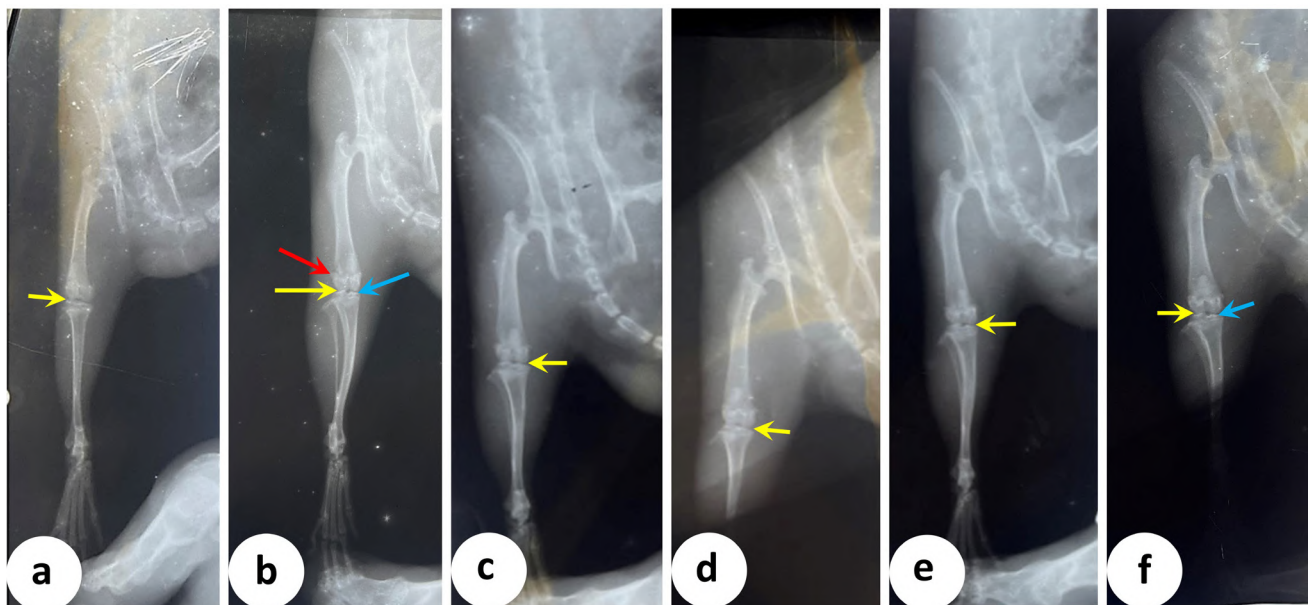


**Fig. 8.** - Radiographs of the rat right knee joint from different groups: **(a)** Control group shows normal tibiofibular joint space (yellow arrow). **(b)** Joint space narrowing (yellow arrow), minute marginal osteophytes (red arrow), irregular tibial articular surface and subchondral sclerosis (blue arrow) are illustrated in OA-induced group. **(c, d, e)** In PRP, BMSCs and concomitant PRP+BMSCs treated groups, there is apparent improvement of joint space (blue arrows) with absence of marginal osteophytes. **(f)** Recovery from MIA reveals narrowing of joint space (yellow arrow), irregular tibial articular surface and subchondral sclerosis (blue arrow).

ginal osteophytes (Figs. 8c, d, e). Recovery from MIA revealed narrowing of the joint space, irregular tibial articular surface and subchondral sclerosis (Fig. 8f).

## DISCUSSION

Osteoarthritis is the most common form of arthritis and one of the leading causes of disability. The knee joint is the most affected joint (Mora et al., 2018). The present study aimed to determine whether PRP can improve the beneficial effect produced by BMSCs for AC repair after OA induction by comparing the therapeutic effect of combined BMSCs and PRP treatment with the PRP and BMSCs alone.

In the current study, examination of rat AC from OA-induced group showed disorganization of chondrocytes, loss of zonation, pyknotic nuclei and empty lacunae. There was a significant decrease in AC thickness compared to control and sham groups. These findings were consistent with Gamal et al. (2019), who induced OA surgically through cartilaginous defect in the rat knee joint. The decrease in AC thickness could be attributed to chondrocyte death and loss of matrix, as suggested by Guzman et al. (2003). Another

pathological alteration in the AC from OA-induced group was the significant decrease in chondrocytes count with subsequent diminution of proteoglycan production. This was confirmed by the significant decrease in the optical density of proteoglycan content compared to control and sham groups. Similar findings were reported by Zare et al. (2020), who studied the proteoglycan content in chondrocytes using toluidine blue stain after induction of OA by intraarticular injection of collagenase type II.

The significant decrease in chondrocytes count and proteoglycan in OA-treated group in the current work was associated with downregulation in ACAN gene expression. In agreement with this result, Dranitsina et al. (2019) reported that ACAN gene expression level decreased two times against control after intra-articular injection of MIA. It was reported that ACAN gene provides instructions for making aggrecan, which is a type of proteoglycan that binds collagen II fibrils and retains water, providing osmosis necessary for the normal function of cartilage (Stöve et al., 2001). Largo et al. (2010) suggested that in OA, oxidative stress leads to chondrocytes death with subsequent decrease in ACAN gene expression and proteoglycan.

The matrix of AC in OA-induced group in the present work showed mild to moderate basophilic staining by Masson's trichrome indicating decreased collagen. This result was consistent with Marino-Martínez et al. (2019), who suggested that necrosis of cartilage cells by OA leads to collagen decrease from the matrix. Furthermore, a significant decrease in the mean area percent of collagen II was found in OA-induced group in this study compared to control and sham groups. A similar finding was mentioned by Zhou et al. (2019) in their study on surgically induced rat knee OA.

Recent research by Ahmad et al. (2020) has shown the important role of inflammation in the pathogenesis of OA. The authors hypothesized that IL-6 is a crucial inflammatory mediator that modulates metalloproteinase activity with subsequent destruction of cartilage in OA. In the present work, degenerative changes in OA-induced group were associated with a significant increase in serum IL-6 level compared to control and sham groups. Similar results were reported by Bastos et al. (2020), who found an increase in the level of IL-6 in the serum of patients with OA.

In the present work, histomorphological improvement was observed in AC from PRP-treated group, apart from disorganization of chondrocytes in the deep zone and absent tidemark. In contrast, Gamal et al. (2019) reported complete zonal organization with clearly seen tidemark. The improvement found in PRP-treated group in this study was associated with a significant increase in chondrocytes count and cartilage height. This was in accordance with Asjid et al. (2019), who proposed that the increase in chondrocyte count was due to the inhibitory effect of PRP on chondrocytes apoptosis.

In addition, a significant increase in the mean optical density of proteoglycan content with increase in ACAN gene expression was observed after PRP administration in the present work compared to OA-induced group. Similarly, Gamal et al. (2019), examined proteoglycan content using toluidine blue stain and found significant increase after adding PRP to osteoarthritic rat knee joint.

It was reported that PRP has anti-inflammatory properties, as it decreases inflammation and ac-

celerates the healing process (Ameer et al., 2018). This was evident in the current study by the significant decrease in serum IL-6 level in PRP-treated group compared to OA-induced group. Similarly, Moussa et al. (2017) used human osteoarthritic chondrocytes, which were co-cultured with an increasing concentration of PRP, and reported significant decrease in IL-6 expression in PRP-treated chondrocytes in a dose dependent manner. The potential therapeutic effect of PRP was also attributed to its ability to inhibit the catabolic effect of MIA or stimulate the anabolic response of the damaged cartilage (Dhillon et al., 2014).

Regarding BMSCs-treated group in the current study, well organized chondrocytes with clearly demarcated tidemark were observed, aside from absent columns in the deep zone of AC. A significant increase in AC thickness was found compared to OA-treated group. In agreement with these findings, Zhou et al. (2019) reported that AC thickness increased significantly, and cartilage degradation apparently decreased after MSCs administration in surgically induced rat knee OA. Moreover, the proteoglycan content and ACAN gene expression level in BMSCs-treated group in the present work increased significantly compared to OA-treated group, which agreed with Latief et al. (2016) and Chen et al. (2019). Those authors used Safranin O stain to detect proteoglycan content of chondrocytes in their studies on animal models of OA. Compared to OA-induced group, treatment by BMSCs in the present study showed a significant increase in the mean optical density of collagen and collagen II in Masson's trichrome and collagen II-stained sections respectively. Similar observations were reported by Zhou et al. (2019) and Kim et al. (2021).

Bastos et al. (2020) attributed the therapeutic effect of MSCs to both their anti-inflammatory activity and the multilineage differentiation. This was confirmed in the present study by the significant decrease in IL-6 in the serum of rats in BMSCs-treated group compared to OA-induced group. In agreement to these findings, a significant decrease in IL-6 after treatment of OA model by MSCs was reported by Zhou et al. (2019).

It was reported that combinational therapy in OA is becoming a popular method for cartilage

repair (Ahmad et al., 2020). In the present work, concomitant PRP+BMSCs administration showed better AC surface continuity and integrity with well-organized three zones of AC. A significant increase in chondrocytes count and proteoglycan content was found in this group compared to either PRP or BMSCs treated group alone. Similar findings were observed by Nabavizadeh et al. (2022), who hypothesized that PRP reinforces the beneficial impacts of MSCs. The significant increase in proteoglycan content in combined group in this study was accompanied by upregulation in ACAN gene level compared to PRP and BMSCs treated groups, which agreed with Ahmad et al. (2020). It was suggested that adding PRP to MSCs decreases cartilage degradation and accelerates OA repair through the release of pro-angiogenic factors, which mobilize the circulation and improve the subchondral bone vasculature (Fahy et al., 2018). In addition, Li et al. (2016) reported that PRP forms a gel, which acts as a scaffold to hold stem cells and helps in the sustained release of growth factors.

The collagen content of the matrix in combined PRP+ BMSCS treated group in the current work showed a significant increase in the optical density of Masson trichrome stained and collagen II-stained sections in comparison to PRP and BMSCs groups. Similar results were reported by Ahmad et al. (2020), who used PRP and adipose-derived MSCs, both in combination and separately in the treatment of surgically induced OA in rats. Another study by Nabavizadeh et al. (2022) revealed a significant increase in collagen II after adding PRP to the used MSCs. Mifune et al. (2013) found a significant increase in collagen II immunostaining in MSCs+PRP compared to PRP treated groups. However, the difference between MSCs+PRP and MSCs groups was non-significant. This might be attributed to the type of stem cells they used in their research (mesenchymal stem cells), although they used the same dose and duration as the present study.

Chen et al. (2014) proposed that adding PRP to MSCs induces chondrogenesis by inhibition of inflammation. The current study revealed that concomitant PRP+BMSCs administration was superior to either PRP or BMSCs treatment alone in

reducing IL-6 level indicating better anti-inflammatory effect of combined therapy. These results were in accordance with Ahmad et al. (2020). In a contradicting study, Bastos et al. (2020) reported a non-significant difference in human IL-6 level between MSCs, MSCs+PRP and corticosteroid-treated groups. The authors attributed the lack of statistical significance to small sample size and heterogeneity in cytokine levels among donors.

In the present study, worsening of osteoarthritic changes was observed in MIA- recovery group after longer duration without treatment as irregular eroded surface, degenerated chondrocytes and several clefts. Similar results were found by Al-Saffar et al. (2009), who reported that the effect of MIA was a time and dose dependent in which changes have been progressed with more prolonged duration of OA induction. The deterioration in the recovery group in the current work was confirmed by the significant decrease in AC thickness, chondrocytes count, optical density of collagen and proteoglycan content in the matrix compared to OA and treated groups. Similarly, Guzman et al. (2003), observed decreased thickness of the AC 14 days after intra articular injection of MIA. The authors found that this decrease was more evident on day 21 after MIA injection. Furthermore, progression of inflammation in the recovery group in the current work was confirmed by the significant increase of serum IL-6 level compared to other groups. Moreover, a significant decrease in ACAN gene expression was found in this group compared to OA and treatment groups. This result coincided with Zhong et al. (2016), who mentioned that ACAN gene expression showed gradually downregulation with increased severity of OA.

In the current work, radiographs from OA-induced group showed narrowing of joint space, subchondral sclerosis and minute marginal osteophytes. It was reported that reduction of collagen II in OA results in increase of water content and subsequent swelling of AC (Poole, 1993). This might explain narrowing of joint space, which was observed in the radiographs of osteoarthritic rats in the current study. On the other hand, X-rays from PRP, BMSCs and combined treatment

groups revealed improvement of joint space, absence of subchondral sclerosis and absence of osteophytes. These results were in accordance with Nabavizadeh et al. (2022), who reported improvement in the joint space and absence of subchondral sclerosis with concomitant administration of MSCs+PRP. However, those authors reported the presence of osteophytes in this group.

## CONCLUSION

It could be concluded that concomitant therapy of PRP and BMSCs ameliorated the deleterious effects of MIA on the rat knee joint. This was evident by the improved histology, AC thickness, enhanced collagen and proteoglycan contents, along with decreased serum IL-6 as well as increased ACAN gene expression in AC. Cotreatment with PRP and BMSCs showed much better results than using PRP and BMSCs alone, therefore it might be a promising option for repair of cartilage in OA.

**Limitations of the study:** Collagen type I might proliferate because of trauma caused by the manipulation and degeneration of the cartilage. Therefore, evaluation of collagen type I in rat articular cartilage after manipulative procedures could be done in future study.

## ACKNOWLEDGEMENTS

The authors express their gratitude to Dr. Ahmed Abd El-Wahab El- Hussein, M.Sc. of Diagnostic and Interventional Radiology, for his help and cooperation in reading the radiographs.

## REFERENCES

- AHMAD MR, BADAR W, ULLAH KHAN MA, MAHMOOD A, LATIF N, IQBAL T, SLEEM MA (2020) Combination of preconditioned adipose-derived mesenchymal stem cells and platelet-rich plasma improves the repair of osteoarthritis in rat. *Regen Med*, 15(11): 2285-2295.
- ALHADLAQ A, MAO JJ (2004) Mesenchymal stem cells: isolation and therapeutics. *Stem Cells Develop*, 13(4): 436-448.
- AL-SAFFAR FJ, GANABADI S, YAAKUB H, FAKURAZI S (2009) Collagenase and sodium iodoacetate-induced experimental osteoarthritis model in Sprague Dawley rats. *Asian J Sci Res*, 2(4): 167-179.
- AMEER LA, RAHEEM ZJ, ABDULRAZAQ SS, ALI BG, NASSER MM, KHAIRI AWA (2018) The anti-inflammatory effect of the platelet-rich plasma in the periodontal pocket. *Eur J Dent*, 12(04): 528-531.
- ASJID R, FAISAL T, QAMAR K, KHAN SA, KHALIL A, ZIA MS (2019) Platelet-rich plasma-induced inhibition of chondrocyte apoptosis directly affects cartilage thickness in osteoarthritis. *Cureus*, 11(11): 6050-6059.
- AZIZ MA, ATTA HM, MAHFOUZ S, FOUAD HH, ROSHDY NK, AHMED HH, HASAN NM (2007) Therapeutic potential of bone marrow-derived mesenchymal stem cells on experimental liver fibrosis. *Clin Biochem*, 40(12): 893-899.

- BANCROFT JD, GAMBLE M (2008) Theory and Practice of Histological Techniques. 7<sup>th</sup> edition. John Bancroft, Churchill Livingstone, Edinburgh, London, Madrid, New York and Tokyo, pp 147-150.
- BASTOS R, MATHIAS M, ANDRADE R, AMARAL RJ, SCHOTT V, BALDUINO A, ESPREGUEIRA-MENDES J, (2020) Intra-articular injection of culture-expanded mesenchymal stem cells with or without addition of platelet-rich plasma is effective in decreasing pain and symptoms in knee osteoarthritis: a controlled, double-blind clinical trial. *Knee Surg Sports Traumatol Arthrosc*, 28(6): 1989-1999.
- CHEN WH, LO WC, HSU WC, WEI HJ, LIU HY, LEE CH, DENG WP (2014) Synergistic anabolic actions of hyaluronic acid and platelet-rich plasma on cartilage regeneration in osteoarthritis therapy. *Biomaterials*, 35(36): 9599-9607.
- CHEN W, SUN Y, GU X, HAO Y, LIN J, CHEN S (2019) Conditioned medium of mesenchymal stem cells delays Osteoarthritis progression in a rat model by protecting subchondral bone, maintaining matrix homeostasis, and enhancing autophagy. *J Tissue Eng Regen Med*, 13(9): 1618-1628.
- DHILLON MS, BEHERA P, PATEL S, SHETTY V (2014) Orthobiologics and platelet rich plasma. *Indian J Orthop*, 48(1): 1-9.
- DRANITSINA AS, DVORSHCHENKO KO, KOROTKYI OH, VOVK AA, FALALYEYEVA TM, GREBINYK DM, OSTAPCHENKO LI (2019) Expression of Nos2 and Acan genes in rat knee articular cartilage in osteoarthritis. *Cytol Genet*, 53(6): 481-488.
- FAHY N, ALINI M, STODDART MJ (2018) Mechanical stimulation of mesenchymal stem cells: Implications for cartilage tissue engineering. *J Orthop Res*, 36(1): 52-63.
- GAMAL N, ABOU-RABIA NM, EL EBIARY FH, KHALAF G, RAAFAT MH (2019) The possible therapeutic role of platelet rich plasma on a model of osteoarthritis in male albino rat. Histological and immunohistochemical study. *Egypt J Histol*, 42(3): 554-566.
- GUZMAN RE, EVANS MG, BOVE S, MORENKO B, KILGORE K (2003) Mono-iodoacetate-induced histologic changes in subchondral bone and articular cartilage of rat femorotibial joints: an animal model of osteoarthritis. *Toxicol Pathol*, 31(6): 619-624.
- KIERNAN JK (2001) Histological and Histochemical methods: Theory and practice. 3<sup>rd</sup> edition. Arnold Publisher, London, New York and New Delhi, pp 111-162.
- KIM YS, KIM YI, KOH YG (2021) Intra-articular injection of human synovium-derived mesenchymal stem cells in beagles with surgery-induced osteoarthritis. *J Knee*, 28: 159-168.
- KYRIAKOU C, RABIN N, PIZZEY A, NATHWANIA, YONG K (2008) Factors that influence short-term homing of human bone marrow-derived mesenchymal stem cells in a xenogeneic animal model. *Haematologica*, 93(10): 1457-1465.
- LARGO R, ROMAN-BLAS JA, MORENO-RUBIO J, SÁNCHEZ-PERNAUTE O, MARTÍNEZ-CALATRAVA MJ, CASTAÑEDA S, HERRERO-BEAUMONT G (2010) Chondroitin sulfate improves synovitis in rabbits with chronic antigen-induced arthritis. *Osteoarthritis Cartil*, 18(1): S17-S23.
- LATIEF N, RAZA FA, BHATTI FUR, TARAR MN, KHAN SN, RIAZUDDIN S (2016) Adipose stem cells differentiated chondrocytes regenerate damaged cartilage in rat model of osteoarthritis. *Cell Biol Int*, 40(5): 579-588.
- LI H, SUN S, LIU H, CHEN H, RONG X, LOU J, LIU H (2016) Use of a biological reactor and platelet-rich plasma for the construction of tissue-engineered bone to repair articular cartilage defects. *Exp Ther Med*, 12(2): 711-719.
- MARINO-MARTÍNEZ IA, MARTÍNEZ-CASTRO AG, PEÑA-MARTÍNEZ VM, ACOSTA-OLIVO CA, VÍLCHEZ-CAVAZOS F, GUZMÁN-LÓPEZ A, LARA-ARIAS J (2019) Human amniotic membrane intra-articular injection prevents cartilage damage in an osteoarthritis model. *Exp Ther Med*, 17(1): 11-16.
- MATSUMOTO T, COOPER GM, GHARAIBEH B, MESZAROS LB, LI G, USAS A, HUARD J (2009) Cartilage repair in a rat model of osteoarthritis through intraarticular transplantation of muscle-derived stem cells expressing bone morphogenetic protein 4 and soluble Flt-1. *Arthritis Rheum*, 60(5): 1390-1405.
- MEHRANFAR S, ABDI RAD I, MOSTAFAVI E, AKBARZADEH A (2019) The use of stromal vascular fraction (SVF), platelet-rich plasma (PRP) and stem cells in the treatment of osteoarthritis: an overview of clinical trials. *Artif Cells Nanomed Biotechnol*, 47(1): 882- 890.

MIFUNE Y, MATSUMOTO T, TAKAYAMA K, OTA S, LI H, MESZAROS LB, HUARD J (2013) The effect of platelet-rich plasma on the regenerative therapy of muscle derived stem cells for articular cartilage repair. *Osteoarthr Cartil*, 21(1): 175-185.

MORA JC, PRZKORA R, CRUZ-ALMEIDA Y (2018) Knee osteoarthritis: pathophysiology and current treatment modalities. *J Pain Res*, 11: 2189-2196.

MORAIS SV, CZECZKO NG, MALAFAIA O, RIBAS FILHO JM, GARCIA JBS, MIGUEL T, MASSIGNAN AG (2016) Osteoarthritis model induced by intra-articular monosodium iodoacetate in rats knee. *Acta Cir Bras*, 31(11): 765-773.

MOUSSA M, LAJEUNESSE D, HILAL G, EL ATAT O, HAYKAL G, SERHAL R, ALAAEDDIN E (2017) Platelet rich plasma (PRP) induces chondroprotection via increasing autophagy, anti-inflammatory markers, and decreasing apoptosis in human osteoarthritic cartilage. *Exp Cell Res*, 352(1): 146-156.

NABAVIZADEH SS, TALAEI-KHOZANI T, ZAREI M, ZARE S, HOSSEINABADI OK, TANIDEH N, DANESHI S (2022) Attenuation of osteoarthritis progression through intra-articular injection of a combination of synovial membrane-derived MSCs (SMMSCs), platelet-rich plasma (PRP) and conditioned medium (secretome). *J Orthop Surg Res*, 17(1): 1-12.

PEI Y, CUI F, DU X, SHANG G, XIAO W, YANG X, CUI Q (2019) Antioxidative nanofullerol inhibits macrophage activation and development of osteoarthritis in rats. *Int J Nanomed*, 14: 4145-4155.

PITCHER T, SOUSA-VALENTE J, MALCANGIO M (2016) The monoiodoacetate model of osteoarthritis pain in the mouse. *J Vis Exp*, 16(111): 746-756.

POOLE AR (1993) Cartilage in health and disease. In: McCarty DJ, Koopman WJ (eds.). *Arthritis and allied conditions: a textbook of rheumatology*. Lea and Febiger, Philadelphia, pp 279-333.

SAMSONRAJ RM, RAGHUNATH M, NURCOMBE V, HUI JH, VAN WIJNEN AJ, COOL SM (2017) Concise review: multifaceted characterization of human mesenchymal stem cells for use in regenerative medicine. *Stem Cells Transl Med*, 6(12): 2173-2185.

SINGH AS, MASUKU MB (2014) Sampling techniques and determination of sample size in applied statistics research: an overview. *Int J Econ Comm Manag*, 2(11): 1-22.

SMAJILAGIĆ A, ALJIČEVIĆ M, REDŽIĆ A, FILIPOVIĆ S, LAGUMDŽIJA AC (2013) Rat bone marrow stem cells isolation and culture as a bone formative experimental system. *Bosnian J Basic Med Sci*, 13(1): 27-30.

STÖVE J, GERLACH C, HUCH K, GÜNTHER KP, BRENNER R, PUHL W, SCHARF HP (2001) Gene expression of stromelysin and aggrecan in osteoarthritic cartilage. *Pathobiology*, 69(6): 333-338.

ZARE R, TANIDEH N, NIKAHVAL B, MIRTALEBI MS, AHMADI N, ZAREA S, ASHKANI-ESFAHANI S (2020) Are stem cells derived from synovium and fat pad able to treat induced knee osteoarthritis in rats? *Int J Rheumatol*, 2020: 9610261.

ZHONG L, HUANG X, KARPERIEN M, POST JN (2016) Correlation between gene expression and osteoarthritis progression in human. *Int J Mol Sci*, 17(7): 1126-1132.

ZHOU J, WANG Y, LIU Y, ZENG H, XU H, LIAN F (2019) Adipose derived mesenchymal stem cells alleviated osteoarthritis and chondrocyte apoptosis through autophagy inducing. *J Cell Biochem*, 120(2): 2198-2212.